

Compact Multi-Mode Filtering Power Divider with High Selectivity, Improved Stopband and In-band Isolation

Zhenyao Qian, Yuan Chen, Chunmei Feng, and Wei Wang

School of Electrical and Automation Engineering
Nanjing Normal University, Nanjing, 210046, China
wei_wang_nnu@126.com

Abstract — This letter presents a new compact multi-mode filtering power divider (FPD) design based on co-shared FPD topology with sharp frequency selectivity, improved out-of-band harmonic rejection and port-to-port isolation. Power splitting and quasi-elliptic filtering functions are achieved by masterly integrating only one triple-mode resonator. By loading different open-circuited stubs at the input/output ports, multiple additional transmission zeros (TZs) are generated at both lower and upper stopband, resulting in an improved stopband performance. Meanwhile, a better port-to-port isolation is obtained by adopting frequency-dependent resistor-capacitor parallel isolation network. The proposed multi-mode FPD design stands out from those in the literature by both nice operation performance and compact topology with only one resonator. For demonstration purposes, one triple-mode FPD prototype and its improved one are implemented, respectively. Measured results exhibit the superiority of the FPD design.

Index Terms — Compact, filtering power divider, harmonic rejection, isolation.

I. INTRODUCTION

Modern mobile communication systems require the RF front-end system to become more compact and multi-functional. In this context, the concept of filtering power divider (FPD) has emerged. By integrating both filtering function and power division function into singly one circuit, such this component can not only decrease insertion loss and avoid cascading mismatch problems to improve the overall performance of the package system, but also significantly reduce the size. In recent years, some achievements have been made in exploring high-performance FPDs [1-10].

In [1], the FPD is designed by using multiple resistors coupled output structures. Although this design achieves well isolation, its return loss (RL) is not satisfactory. In [2], the coupled-resonator circuit theory is utilized to guide narrow band FPD designs. However,

its port-to-port isolation performance and its overall size are not ideal. In [7], using two resonators to achieve well two-way power divider filtering performance. However, the adopted topology results in a relatively large size. In order to improve the above operation performance, other discriminating couplings [3], mixed electric and magnetic couplings [4], radial/rectangular-shaped resonators and Ring Resonators [5-6], quarter-wavelength transmission lines [8], and Parallel-Coupled Line Structures [9] are also employed in different power divider configurations, respectively. For good in-band isolation, a coupled line isolation network consisting of a resistor and a capacitor connected in series is put forward in [10]. However, the above series connection results in the design difficulty.

The main intention of the paper is to propose a compact high-performance multi-mode filtering power divider design. By embedding different open-circuited stubs and frequency-dependent resistor-capacitor parallel isolation network into just one triple-mode resonator based design, the proposed FPD exhibits compact size, high selectivity, improved lower/upper stopband and increased in-band isolation performance. To validate the design concept and method, two prototypes including the first presented FPD and its improved one are designed and implemented, respectively. Measured results validate the design concept.

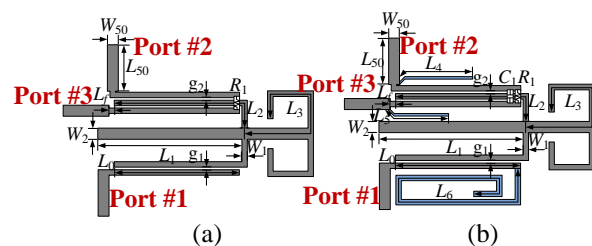


Fig. 1. Configuration of the proposed filtering power dividers. (a) The first presented FPD; (b) the improved FPD. (Substrate Rogers RO4003C: $\epsilon_{re}=3.55$, $\tan\delta=0.0027$, and $h=0.508$ mm).

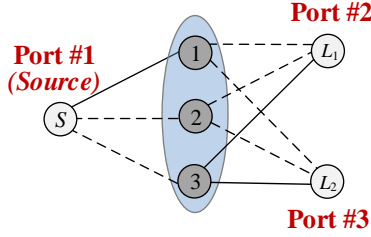


Fig. 2. The design coupling topology of the proposed FPDs.

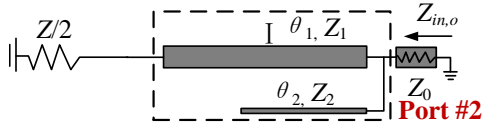


Fig. 3. Equivalent circuit for odd excitation of the improved FPD.

II. PROPOSED FPDs DESIGN

These two prototypes are presented with the structures illustrated in Figs. 1 (a) and (b). The first presented FPD is mainly constructed by only one cross-shaped resonator and one resistor. By elaborately attaching one open-circuited stub at input line and two at output coupled lines, and loading one frequency-dependent capacitor with isolation resistor in parallel, the improved FPD is constructed. With the above loaded stubs, more favorable filtering response is achieved. Simultaneously, the improved isolation network further improves the in-band isolation flexibly and effectively.

For the configurations in Fig. 1, the input signal excited by the source (Port #1) will be coupled to the multi-mode resonator, and then equally divided to the feed-lines of the output ports through another arm of the resonator. The design coupling topology is shown in Fig. 2, where the light gray disks S and L_p ($p=1, 2, 3$) denote source and loads while dark gray disks 1-3 represent the three modes of the resonator. Since the coupling topology is symmetrical, the isolation network hardly affects the filtering responses [11] and thereby not yet being considered in Fig. 2.

As the proposed structure is symmetric, its resonance characteristic can be analyzed by making use of even-/odd-mode analysis method [11-12]. The standard scattering parameters of the proposed filtering power divider in Fig. 1 can be calculated as [11]:

$$S_{11} = S_{11e}, \quad (1a)$$

$$S_{21} = S_{31} = \frac{S_{21e}}{\sqrt{2}}, \quad (1b)$$

$$S_{23} = \frac{(S_{22e} - S_{22o})}{2}, \quad (1c)$$

$$S_{22} = S_{33} = \frac{(S_{22e} + S_{22o})}{2}, \quad (1d)$$

According to the design principles (1a)-(1d) of the filtering power divider in the manuscript, idea filtering response can be determined at first, then in order to achieve good matching and isolation for output ports, equivalent circuit for odd excitation of the improved FPD can be analyzed. Detailed analysis is given in the followings.

According to the prescribed specifications ($f_0=2.5$ GHz, ripple bandwidth of 0.33 GHz, the passband return loss of 20 dB), the targeted coupling matrix coefficients is synthesized with the analysis method in [11] as: $M_{S1} = M_{L1} = 0.4465$, $M_{S2} = -M_{L2} = -0.8374$, $M_{S3} = M_{L3} = 0.4552$, $M_{11} = 1.3933$, $M_{22} = 0.0165$, $M_{33} = -1.4006$. Based on equation (2), the required even-mode resonant frequencies (f_{e1}, f_{e2}) and odd-mode resonant frequency f_o of the multi-mode resonator (MMR) can be derived as $f_{e1} = 2.27$ GHz, $f_o = 2.49$ GHz and $f_{e2} = 2.73$ GHz. With the help of the derived resonant frequencies, the physical dimension of MMR can be determined:

$$f_n = \frac{f_0}{2} \cdot \left[\frac{-BW}{f_0} M_{ii} + \sqrt{\left(\frac{BW}{f_0} M_{ii}\right)^2 + 4} \right], i=1, 2, 3; n=e1, o, e2. \quad (2)$$

The I/O couplings to even- and odd-modes can be characterized in terms of external quality factors Q_{e-n} ($n=e1, o, e2$), which are found from $Q_{e-n} = f_0 / (BW \cdot M_{si}^2)$ as: $Q_{e-e1}=37.8$, $Q_{e-o}=10.5$, $Q_{e-e2}=36.4$. Based on these derived external quality factors, the width ($W_1=0.6$ mm) and gap ($g_1=0.1$ mm and $g_2=0.25$ mm) can be determined by extracting the I/O couplings from $Q_{e-n} = \pi f_i \cdot \tau(f_i)$ through the group delays as in [12].

Next, once the filtering response is determined, the port-to-port isolation and matching can be fulfilled by changing the isolation network of the odd mode equivalent circuit as shown in Fig. 3. Z can then be derived with odd mode equivalent circuit. The input impedance is then calculated as:

$$Z_{in,oo} = \frac{AZ + B}{CZ + D} = Z_0, \quad (3)$$

where A, B, C, D are the elements of the transmission matrix $[A]$ for block I, which are derived as follows:

$$[A] = \begin{bmatrix} \cos \theta_1 & j4Z_1 \sin \theta_1 \\ j\left(\frac{1}{4Z_1}\right) \sin \theta_1 & \cos \theta_1 \end{bmatrix} \cdot \begin{bmatrix} 1 & 0 \\ \frac{1}{Z_2} & 1 \end{bmatrix}, \quad (4)$$

where Z_1 and θ_1 are the impedance and electrical length for the transmission line as shown in Fig. 3.

Thus, Z can be calculated as $162+j532$, in other words, R_1 and C_1 are calculated as 162 and 0.12 pF. Figure 4 plot the theoretical results on the in-band isolation versus the value of the parallel resistor and the capacitor.

Secondly, to clarify the design procedure of the proposal, the detailed design steps are described for explanation.

1) Firstly, according to the given specifications, the targeted coupling matrix coefficients is synthesized.

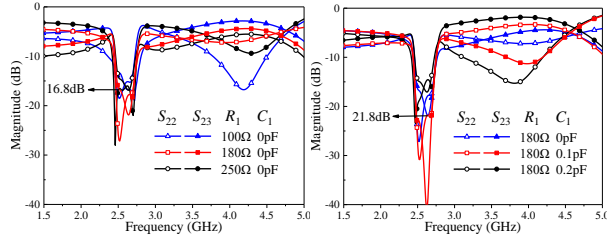


Fig. 4. The corresponding S-parameters S_{22} and S_{23} with varied R_1 and C_1 .

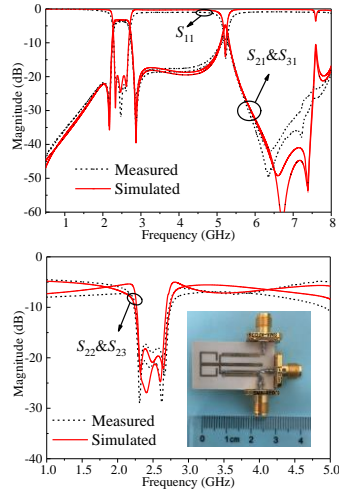


Fig. 5. The operation performance for the first presented FPD.

Based on equation (2), the required resonant frequencies of the multi-mode resonator (MMR) can be derived as $f_{e1} = 2.27$ GHz, $f_o = 2.49$ GHz and $f_{e2} = 2.73$ GHz. With the help of the derived resonant frequencies, the physical dimension of MMR can be determined.

2) Subsequently, determine the input/output coupling space (g) and feedline width (w) by extracting the group delays based on the formulas $Q_{e-n} = f_o / (BW \cdot M_{si}^2)$ and $Q_{e-n} = \pi f_i \cdot \tau(f_i)$. The first FPD is initially designed and fine-tuned to achieve optimal filtering response.

3) Next, determine initial isolation network to achieve favorable port matching and port-port isolation.

4) Finally, execute the final optimization of the realized entire circuit layout relying on the commercial EM simulator HFSS.

For demonstration, the layouts of the proposed FPDs shown in Figs. 1 (a) and (b) were simulated,

fabricated and measured. The images of the fabricated FPDs are exhibited in the insert plot of Fig. 5 and Fig. 6.

The final parameters are determined as follows (Units: mm): $L_0=14.45$, $L_1=15.8$, $L_2=17.85$, $L_3=19.8$, $L_f=0.7$, $L_{50}=5$, $W_{50}=1.18$, $W_1=0.6$, $W_2=1.2$, $g_1=0.1$, $g_2=0.25$, $R_1=140\Omega$. The size of the design circuit is about $0.32\lambda_g \times 0.12\lambda_g$, where λ_g is the guided wavelength at the center frequency. Figure 5 shows the simulated and measured results, indicating the first presented FPD operates at the center frequency of 2.48 GHz with a 3-dB fractional bandwidth (FBW) of 17.3%. As expected, two inherent TZs are created due to the virtual grounds existing in the resonators. Within the passband, the measured input return loss (RL) is better than 20.5 dB and the output port RLs are better than 20.5 dB, while the insertion loss (IL) is smaller than 0.8 dB, respectively. The measured port-to-port isolations is higher than 17.3 dB.

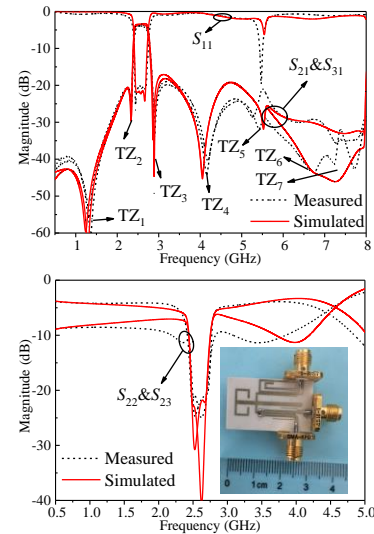


Fig. 6. The operation performance for the second presented FPD.

As for the improved one in Fig. 1 (b), the optimal layout parameters are finally determined as follows (Units: mm): $L_0=13.5$, $L_1=15.7$, $L_2=16.9$, $L_3=18$, $L_4=8$, $L_5=6.4$, $L_6=34.7$, $L_f=0.7$, $L_{50}=5$, $W_{50}=1.18$, $W_1=0.6$, $W_2=1.2$, $g_1=0.1$, $g_2=0.25$, $R_1=180\Omega$ and $C_1=0.1\text{pF}$. The size of the design circuit is about $0.33\lambda_g \times 0.18\lambda_g$. Figure 6 shows the simulated and measured results. As observed from the figure, the measured center frequency is 2.6 GHz with the 3-dB FBW of 13.2%. The corresponding measured in-band IL of the FPD is 0.8 dB, and the input RL is better than 20.0 dB, respectively. Additionally, the RLs at the output ports are better than 21.0 dB while the port-to-port isolations are higher than 21.1 dB. It is worthy noting that seven generated TZs achieve high frequency selectivity and a better than 20 dB harmonic suppression

from DC to 8.0 GHz ($3.1f_0$). The additional $3\lambda_{g1}/4$ folded open-circuited stub loaded at the input line can introduce two additional TZs (TZ₁ and TZ₄) as showed in Fig. 6. The lengths of loaded open-circuited stubs at output lines mainly determine the position of the fifth TZ as indicated in Fig. 6. The relationship between the position of the TZ_n (n=1, 4, 5) and the electrical length of the loaded stubs

lengths of loaded open-circuited stubs at output lines mainly determine the position of the fifth TZ as indicated in Fig. 6. The relationship between the position of the TZ_n (n=1, 4, 5) and the electrical length of the loaded stubs (θ_{stub}) can be expressed as:

$$f_{z1/4/5} = \frac{f_0}{\theta_{stub}} \left(\frac{\pi}{2} + k\pi \right), k = 0, 1, 2, \dots \quad (5)$$

Table 1: Performance comparisons with other reported works

Ref.	Insertion Loss	Input Return Loss	Output Return Loss	In-band Isolation	TZs	Number-way	Topology	Dimension ($\lambda_g \times \lambda_g$)	Suppression
[1]	0.74 dB	10.0 dB	12.0 dB	20.0 dB	3	Two-way	Two Double Resonator	0.33×0.25	No
[2]	0.9 dB	17.0 dB	Not given	15.5 dB	4	Two-way	Two Double Resonator	0.89×0.29	Yes
[3]	1.3 dB	15.0 dB	22 dB	16.0 dB	2	Two-way	Four Double Resonator	0.19×0.13	Yes
[7]	1.1 dB	17.0 dB	Not given	21.0 dB	6	Two-way	Two Double Resonator	0.67×0.35	Yes
Work-I	0.8 dB	20.5 dB	20.5 dB	17.3 dB	4	Two-way	Co-shared Single Resonator	0.32×0.12	No
Improved work- II	0.8 dB	20.0 dB	21.0 dB	21.1 dB	7	Two-way	Co-shared Single Resonator	0.33×0.18	Yes

Table 1 illustrates the comparison of the performances of this work with other state-of-the-art FPDs. It indicates that the proposed improved FPD have advantages of nice port matching, sharp frequency selectivity, superior in-band isolation and wide stopband performance. Furthermore, compared with other counterparts, the proposed designs exhibit a very flexible topology and competitive compactness against others.

VI. CONCLUSION

In this letter, a new compact multi-mode filtering power divider (FPD) design has been presented based on co-shared multi-mode coupling topology. It exhibits nice return loss, sharp passband skirt, as well as decent in-band isolation. An improved design is for high port-to-port isolation and wider stopband is realized by loading the additional open-circuited stubs and modifying isolation network. The high port-to-port isolations greater than 21.1 dB and 20-dB harmonic suppression from DC to 8.0 GHz ($3.1f_0$) are obtained. It is believed that the presented FPD design is promising in many practical modern wireless and mobile communication system applications.

ACKNOWLEDGMENT

This work was supported in part by National Natural Science Foundation of China under Grant 61801226, International Science and Technology Cooperation Program of Jiangsu Province and Universities Natural Science Research General Project under Grant BZ2018027 and Grant 18KJB510021, National Natural Science Foundation of China under Grant 61801226,

State Key Laboratory of Millimeter Waves under Grant K201922 and Postgraduate Research & Practice Innovation Program of Jiangsu Province under Grant SJCX18_0369.

REFERENCES

- [1] Y. Wang, F. Xiao, Y. Cao, Y. Zhang, and X. Tang, "Novel wideband microstrip filtering power divider using multiple resistors for port isolation," *IEEE Access*, vol. 7, pp. 61868-61873, May 2019.
- [2] Y. Deng, Y. He, and J. Wang, "Design of a compact wideband filtering power divider with improved isolation," *The Applied Computational Electromagnetics Society Journal*, vol. 31, no. 9, pp. 1079-1083, Sep. 2016.
- [3] X.-L. Zhao, L. Gao, X. Y. Zhang, and J.-X. Xu, "Novel filtering power divider with Wide stopband using discriminating coupling," *IEEE Microwave and Wireless Components Letters*, vol. 26, no. 8, pp. 580-582, Aug. 2016.
- [4] G. Zhang, X. Wang, J. Hong, and J. Yang, "A high-performance dual-mode filtering power," *IEEE Microwave and Wireless Components Letters*, vol. 28, no. 2, pp. 120-122, Feb. 2018.
- [5] R. Pouryavar, F. Shama, and M. A. Imani, "A miniaturized microstrip Wilkinson power divider with harmonics suppression using radial/rectangular-shaped resonators," *Electromagnetics*, vol. 38, no. 2, pp. 113-122, 2018.
- [6] D. Jiang, Y. Xu, R. Xu, and Z. Shao, "Broad-band power divider based on the novel split ring resonators," *The Applied Computational Electro-*

magnetics Society Journal, vol. 29, no. 2, pp. 157-162, Feb. 2014.

- [7] G. Zhang, J. Wang, L. Zhu, and W. Wu, "Dual-band filtering power divider with high selectivity and good isolation," *IEEE Microwave and Wireless Components Letters*, vol. 26, no. 10, pp. 774-776, Oct. 2016.
- [8] M. A. Imani, F. Shama, M. Alirezapoori, S. Haghiri, and A. Ghadrhan, "Ultra-miniaturized Wilkinson power divider with harmonics suppression for wireless applications," *Journal of Electromagnetic Waves and Applications*, vol. 33, no. 14, pp. 1920-1932, 2019.
- [9] X. Yu, S. Sun, and Y. Liu, "Design of wideband filtering power dividers with harmonic suppression based on the parallel-coupled line structures," *The Applied Computational Electromagnetics Society Journal*, vol. 33, no. 5, pp. 468-475, May 2018.
- [10] C.-J. Chen, "A coupled-line isolation network for the design of filtering power dividers with improved isolation," *IEEE Transactions on Components, Packaging and Manufacturing Technology*, vol. 8, no. 10, pp. 1830-1837, Oct. 2018.
- [11] D. M. Pozar, *Microwave Engineering*. Third edition, Wiley-New York, 2005.
- [12] J. S. Hong and M. J. Lancaster, *Microstrip Filters for RF/Microwave Applications*. Second edition, Wiley-New York, 2001.



Zhenyao Qian received B.S. degree from NJUST, Nanjing, China, in 2017. He is currently working toward the M.Sc. degree in Electromagnetic Field in Nanjing Normal University (NNU), Nanjing, China. His research interest is the design of miniaturized high performance microwave power divider.



Yuan Chen is currently working toward the M.Sc. degree in Electromagnetic Field in Nanjing Normal University (NNU), Nanjing, China. She research interest is the design of miniaturized high performance microwave power divider.



Chunmei Feng is currently working in Electromagnetic Field in Nanjing Normal University (NNU), Nanjing, China. In addition, she serves as the associate dean of the college. Her research interests have mainly been numerical methods of electromagnetic field computation and novel wireless power transfer systems.



Wei Wang was born in Nanjing, China, in 1988. He received the B.S. degree in Electrical Engineering and automation from Jiangnan University, Wuxi, China, in 2011, and the M.S. and Ph.D. degrees in Electrical Engineering from Southeast University, Nanjing, China, in 2013 and 2017, respectively.

He currently works as a Lecturer with the School of Electrical and Automation Engineering, and a Post-doctoral Research Associate with the Post-Doctoral Research Center of Physics, Nanjing Normal University, Nanjing, China. Since 2011, his research interests have mainly been numerical methods of electromagnetic field computation and novel wireless power transfer systems.